Supporting Information for

The CRL3^{gigaxonin} ubiquitin ligase–USP15 pathway governs the destruction of neurofilament proteins

Hyoung-Min Park[a], Ly Le[b], Thao T. Nguyen[c], Ki Hong Nam[d], Alban Ordureau[d], J. Eugene Lee[a], and Thang Van Nguyen[e, 1]

[a]Biometrology Group, Korea Research Institute of Standards and Science, Daejeon 34113, Korea.

[b]Division of Quantum Simulation and Optimization, SandboxAQ, NY 10591, USA.

[c]Gehrke Proteomics Center, Christopher S. Bond Life Sciences Center, University of Missouri-Columbia, Columbia, MO 65211, USA.

[d]Cell Biology Program, Sloan Kettering Institute, Memorial Sloan Kettering Cancer Center, New York, NY 10065, USA.

[e]Center for Precision Medicine, Department of Medicine, University of Missouri, Columbia, MO 65212, USA.

[1]Further information and requests for resources and reagents should be directed to

Thang Van Nguyen (Email: nguyentv@health.missouri.edu)

Supporting Information in this file includes:

Supplemental Figures

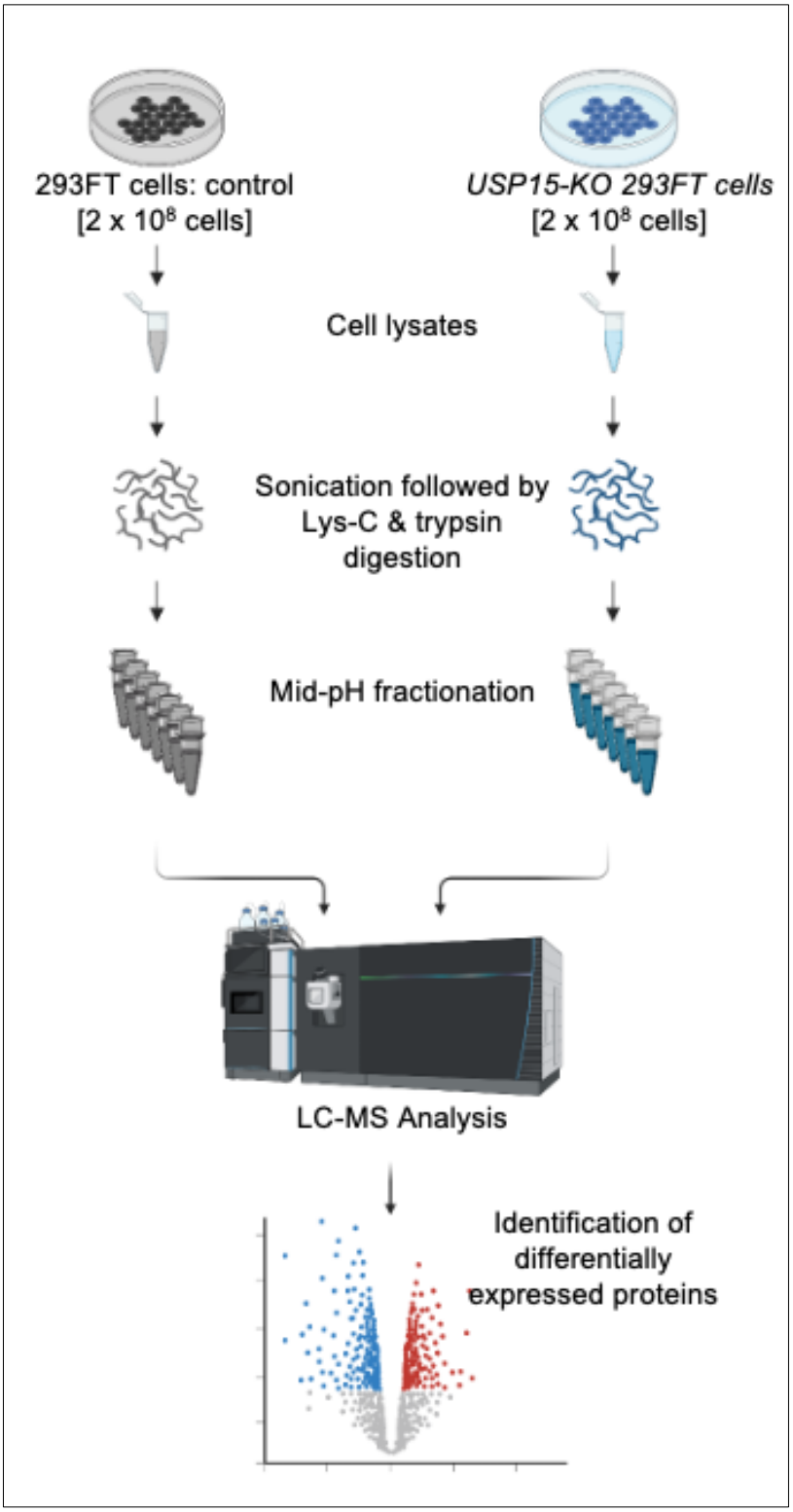

Fig. S1, Related to Fig. 1A. Schematic flow and expression analysis of wild-type and *USP15*-knockout (KO) 293FT cells. 293FT cells and *USP15*-KO 293FT cells were lysed, sonicated, and digested. Digested mixture was fractionated into 7 portions by the mid-pH method, after which the samples were dried for LC-MS analysis.

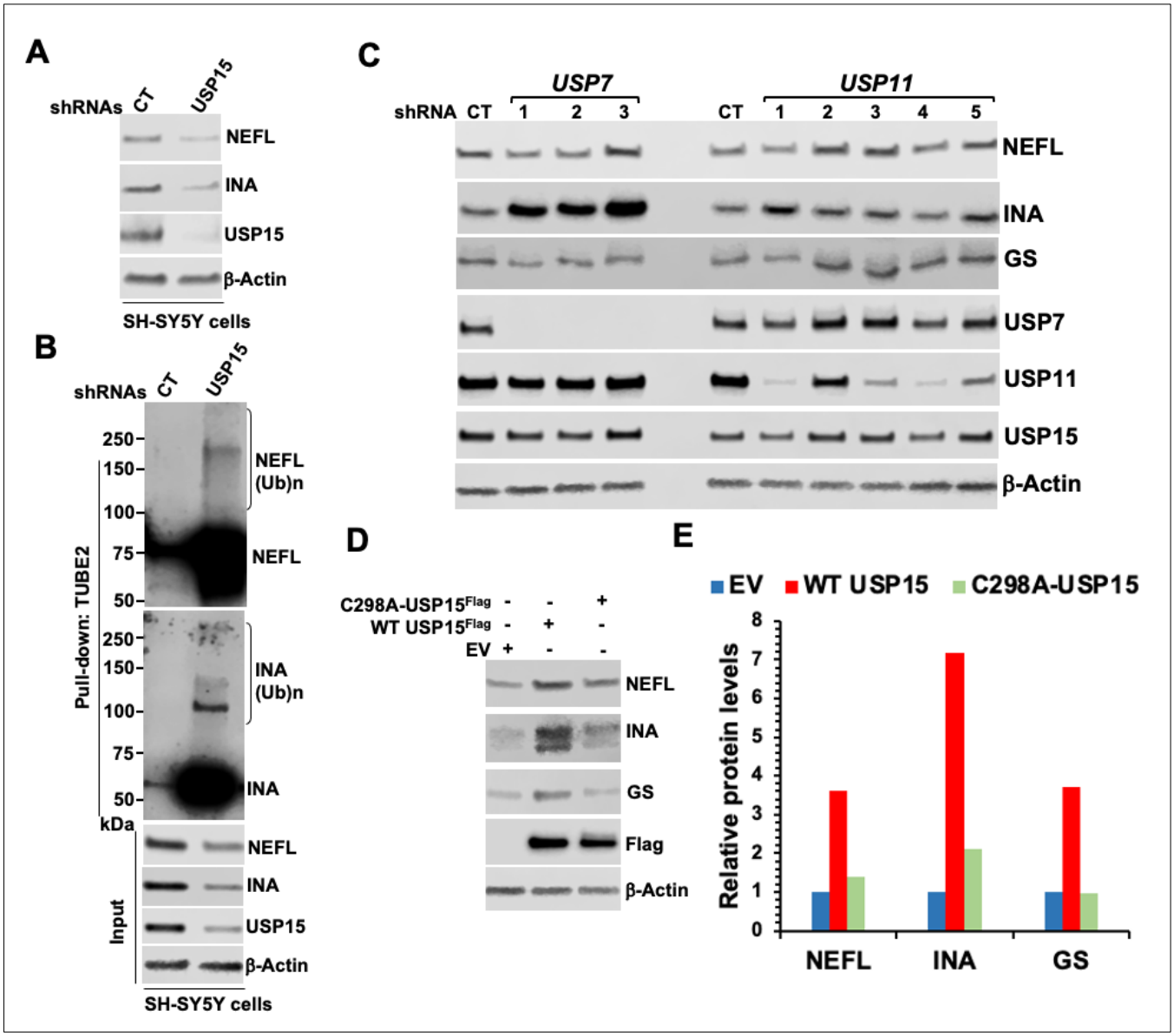

Fig. S2, Related to Fig. 1. USP15 controls the stability of NEFL and INA.
(A) Protein extracts from SH-SY5Y cells, stably expressing non-target shRNA lentivirus (control: CT) or GIPZ lentiviral shRNA targeting human *USP15* clones 4+6, were analyzed by immunoblotting (IB) with the indicated antibodies.
(B) Total ubiquitylated proteins, extracted from SH-SY5Y cells stably expressing non-target shRNA CT or GIPZ lentiviral shRNA targeting human *USP15* clones 4+6, were purified using TUBE2-agarose. Bound fractions and inputs were analyzed by IB. (Ub)n, polyubiquitin.
(C) Protein extracts from 293FT cells, stably transduced with non-target shRNA lentivirus (CT) and GIPZ lentiviral shRNA particles targeting human *USP7* (clones 1-3) and *USP11* (clones 1-5), were analyzed by IB with the indicated antibodies.
(D) *USP15*-KO 293FT cells were transiently transfected with empty vector (EV, control), WT USP15^{Flag} or C298A-USP15^{Flag} mutant plasmid for 48 h. Cell extracts were analyzed by IB with the indicated antibodies. (E) Quantification of NEFL, INA and GS proteins from (D). The results are a representative of at least three independent experiments (A-D).

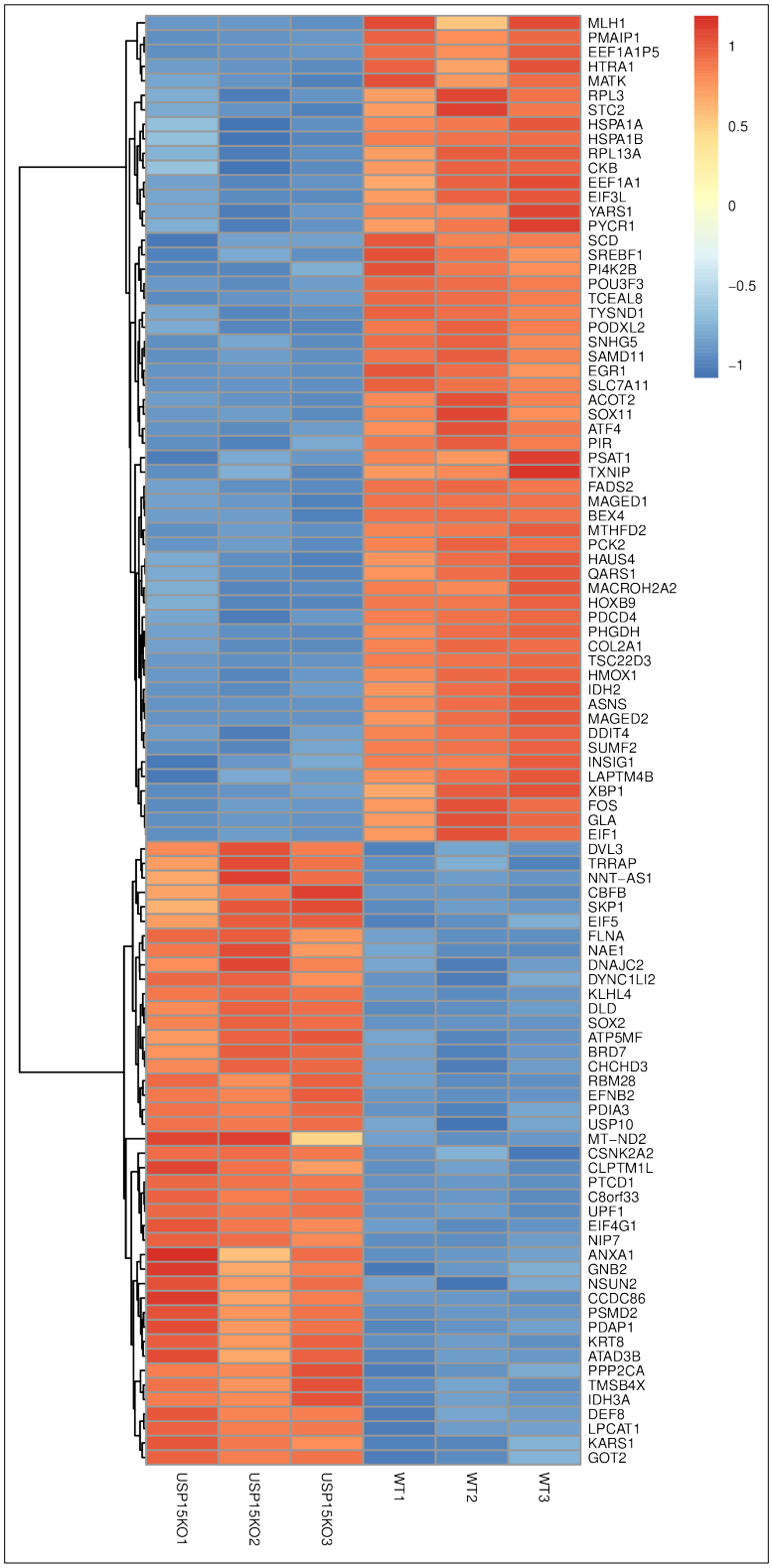

Fig. S3, Related to Fig. 1. Heatmap of differentially expressed genes from RNA-seq (red is higher and blue is lower expression). Relative mRNA levels were the averages of three independent RNA-seq measurements from wild-type 293FT cells (WT1-3) and *USP15*-KO 293FT cells (USP15KO1-3); n = 3.

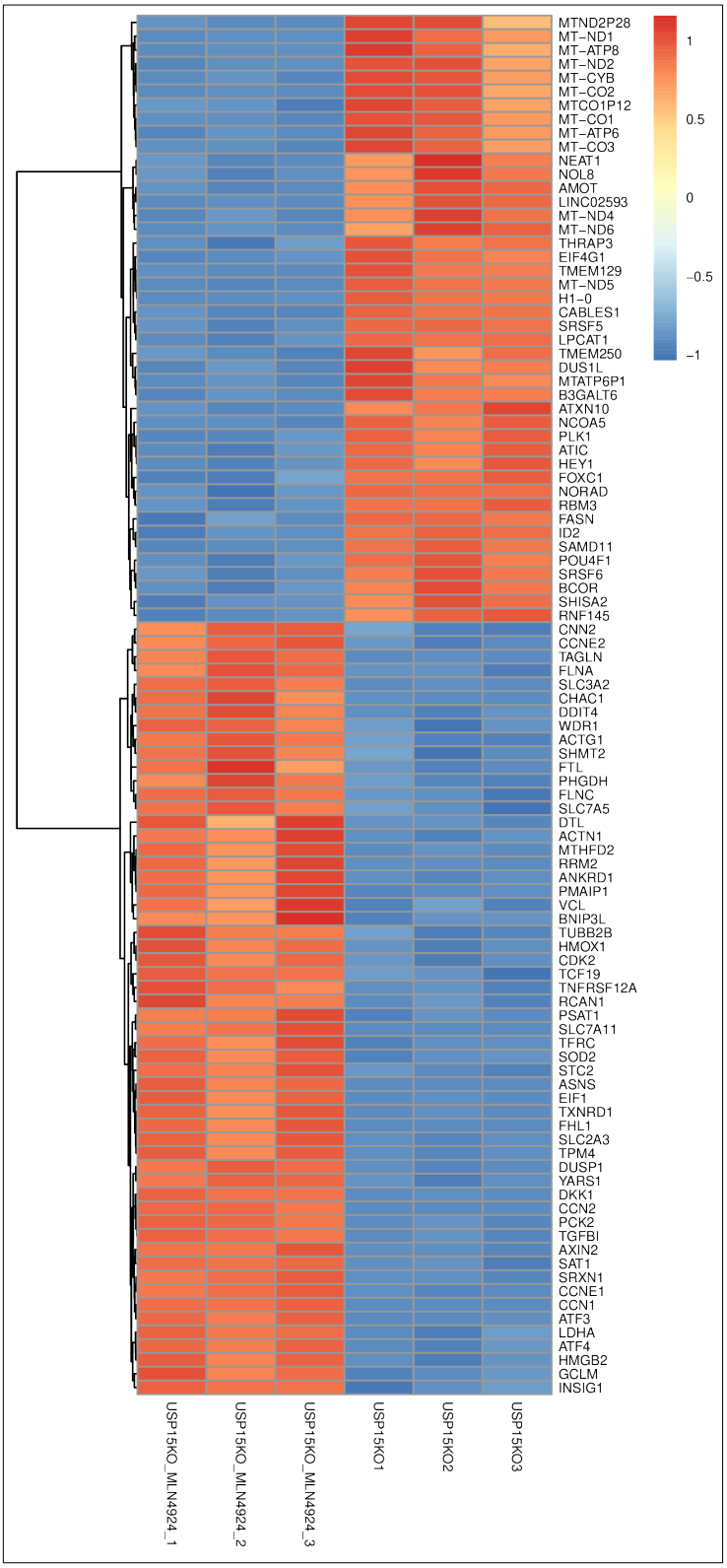

Fig. S4, Related to Fig. 1. Heatmap of differentially expressed genes from RNA-seq (red is higher and blue is lower expression). Relative mRNA levels were the averages of three independent RNA-seq measurements from USP15-KO 293FT cells (USP15KO1-3) and USP15-KO 293FT cells treated with 1 μM MLN4924 for 8 h (USP15KO- MLN4924-1-3); n = 3.

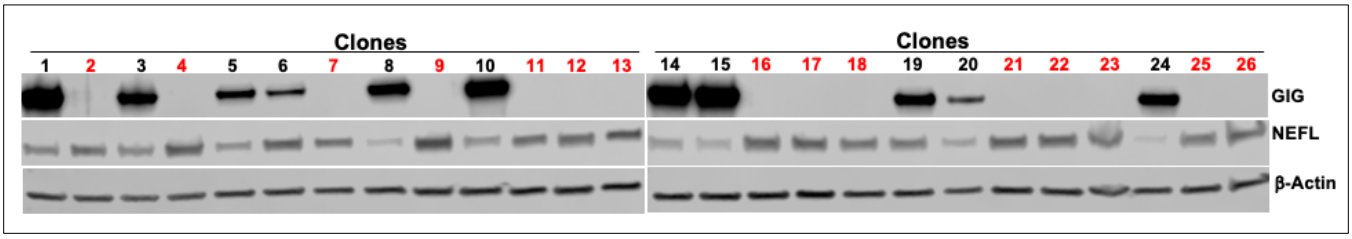

Fig. S5, Related to Fig. 2. Validation of *GAN*-knockout (KO) 293FT cells via CRISPR/Cas9 gene editing. Individual clones of *GAN*-KO 293FT cells were validated by Western blot. Positive *GAN*-KO clones (red) were 2, 4, 7, 9, 11, 12, 13, 16, 17, 18, 21, 22, 23, 25 and 26. *GAN*-KO clones 2 (*GAN*-KO2) and 16 (*GAN*-KO16) were chosen for further analysis. At least three independent experiments were repeated to screen for *GAN*-KO clones.

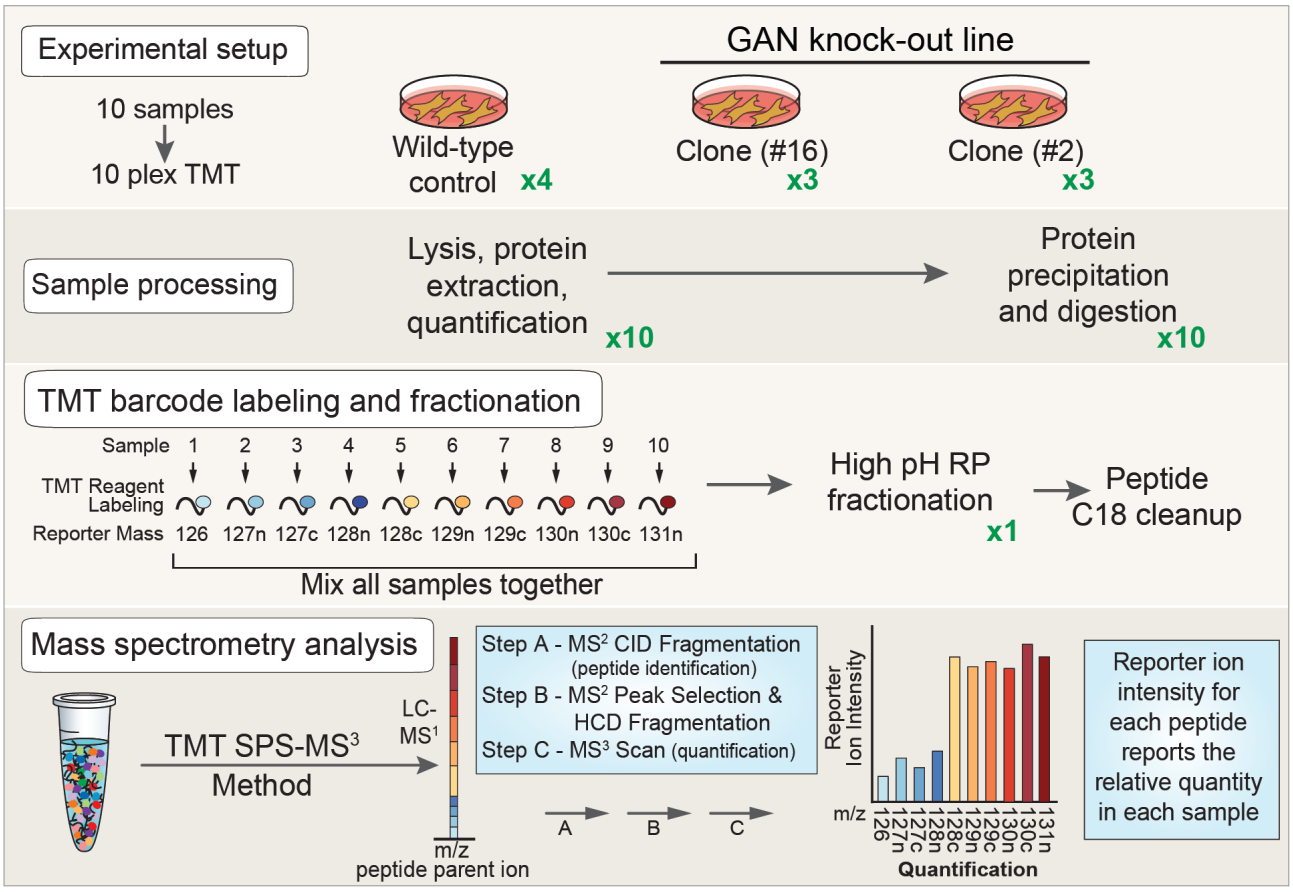

Fig. S6, Related to Fig. 2A. Schematic flow and expression analysis of WT and *GAN*-KO 293FT cell lines using a 10plex Tandem Mass Tag (TMT) workflow. Total cell extracts of WT (4 replicates), and *GAN*-KO2 and *GAN*-KO16 293FT cell lines (triplicate each) were analyzed using multiplexed quantitative proteomics.

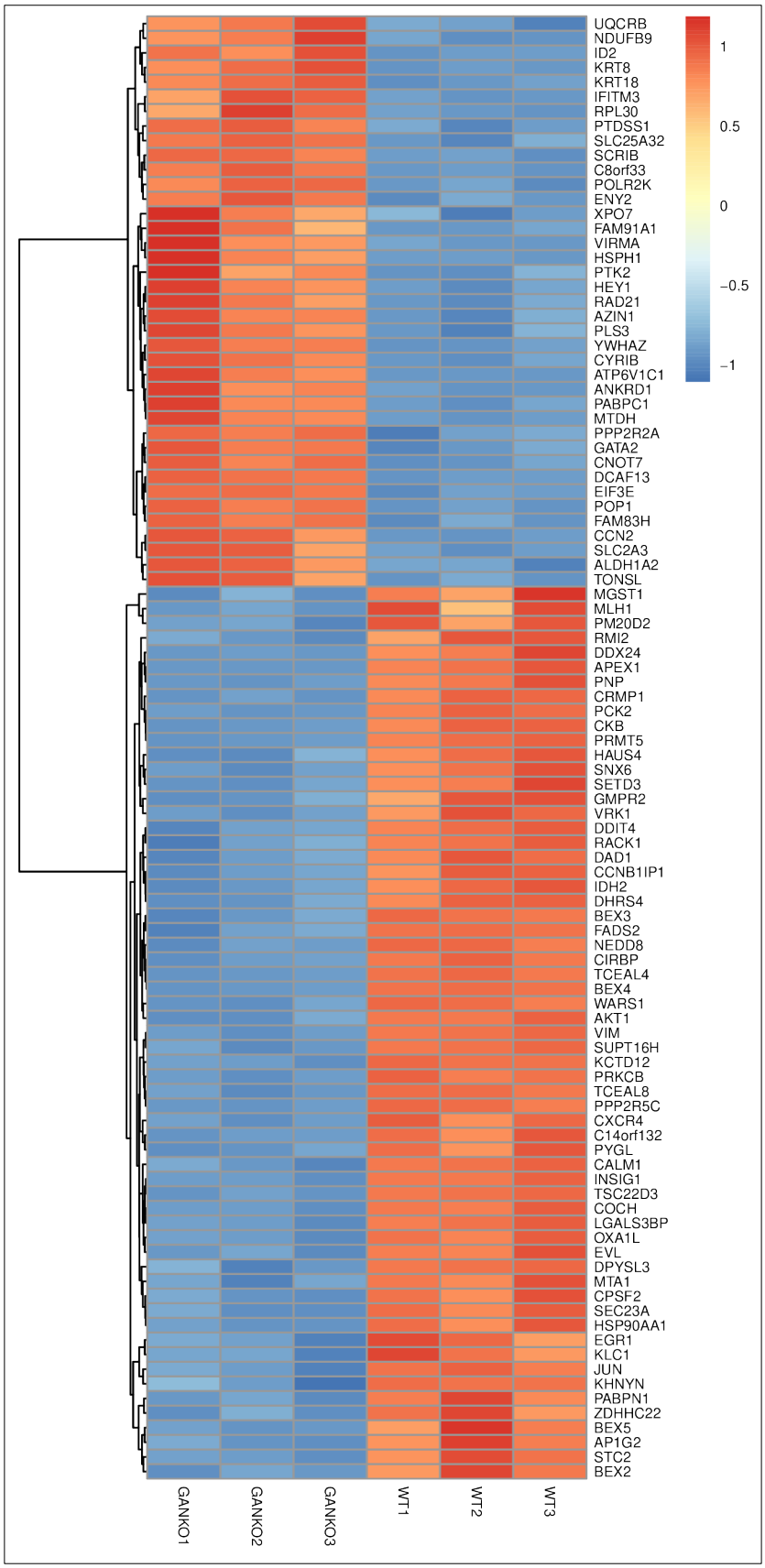

Fig. S7, Related to Fig. 2. Heatmap of differentially expressed genes from RNA-seq (red is higher and blue is lower expression). Relative mRNA levels were the averages of three independent RNA-seq measurements from WT and *GAN*-KO 293FT cell lines; n = 3.

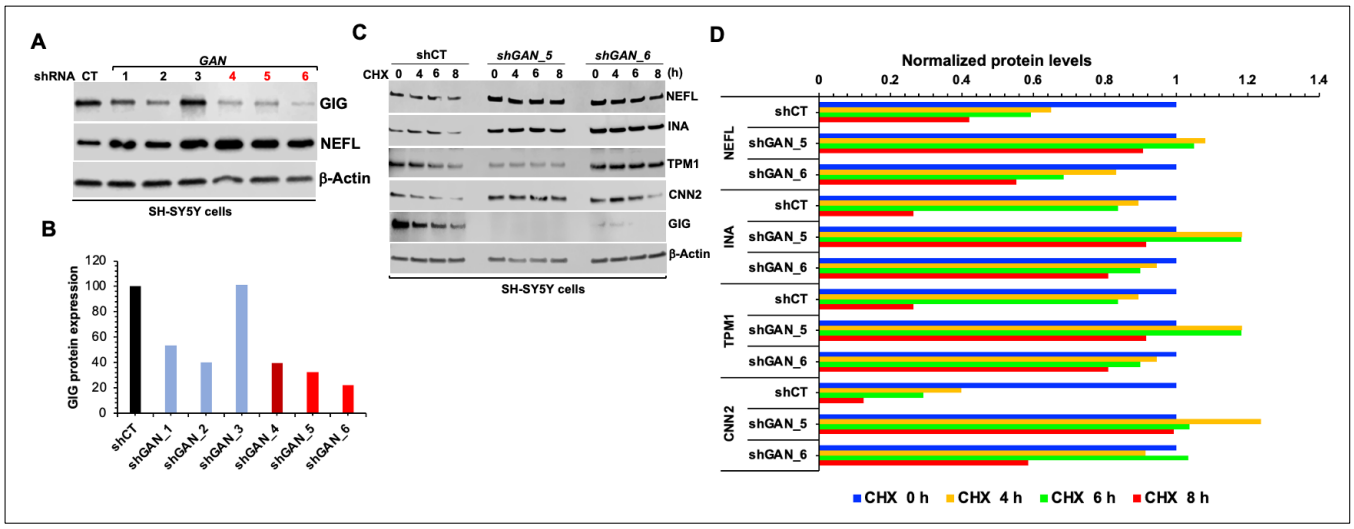

Fig. S8, Related to Fig. 2. The human SH-SY5Y neuroblastoma cell line was used as a neuronal cell model.

(A-B) Validation of *GAN* depletion by lentiviral GIPZ shRNAs in SH-SY5Y cells. (A) Cells were transduced with non-target shRNA lentivirus (control: CT), or GIPZ lentiviral shRNA particles targeting human *GAN*. After 1 week of puromycin selection (at a high dose of 4 μg/ml), protein extracts were analyzed by IB with the indicated antibodies. Among six tested *GAN* shRNAs, clones 4, 5 and 6 (sh*GAN*_5, sh*GAN*_5 and sh*GAN*_6) each exhibiting at least 70 to 80% knockdown compared to non-target shRNA CT, were chosen for further analysis, and used in all subsequent experiments. (B) Quantification of GIG protein from (A).

(C) SH-SY5Y cells, expressing shRNA CT (shCT) and shRNAs targeting *GAN* clones 5 and 6 (shGAN_5, shGAN_6), were treated with CHX for the indicated times. Cell extracts were analyzed by IB with the indicated antibodies. (D) Quantification of NEFL, INA, TPM1 and CNN2 proteins from (C). Representative Western Blots were shown in A and C; n = 3.

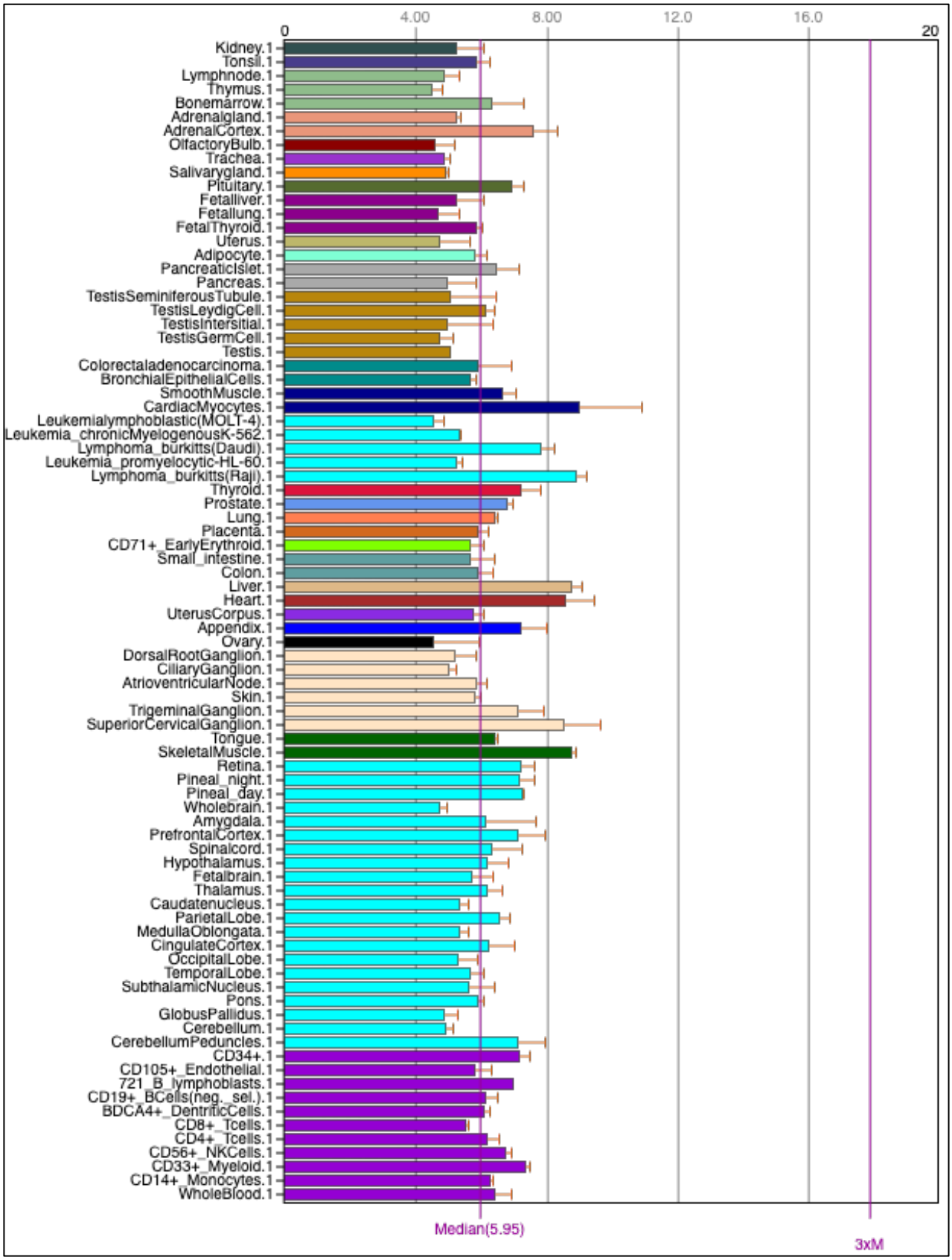

Fig. S9, Related to Fig. 2. GAN **is highly transcribed in heart, liver, kidney, skeletal muscle, and brain.** *GAN* mRNA expression profile in diverse human tissues reported at BioGPS.org.

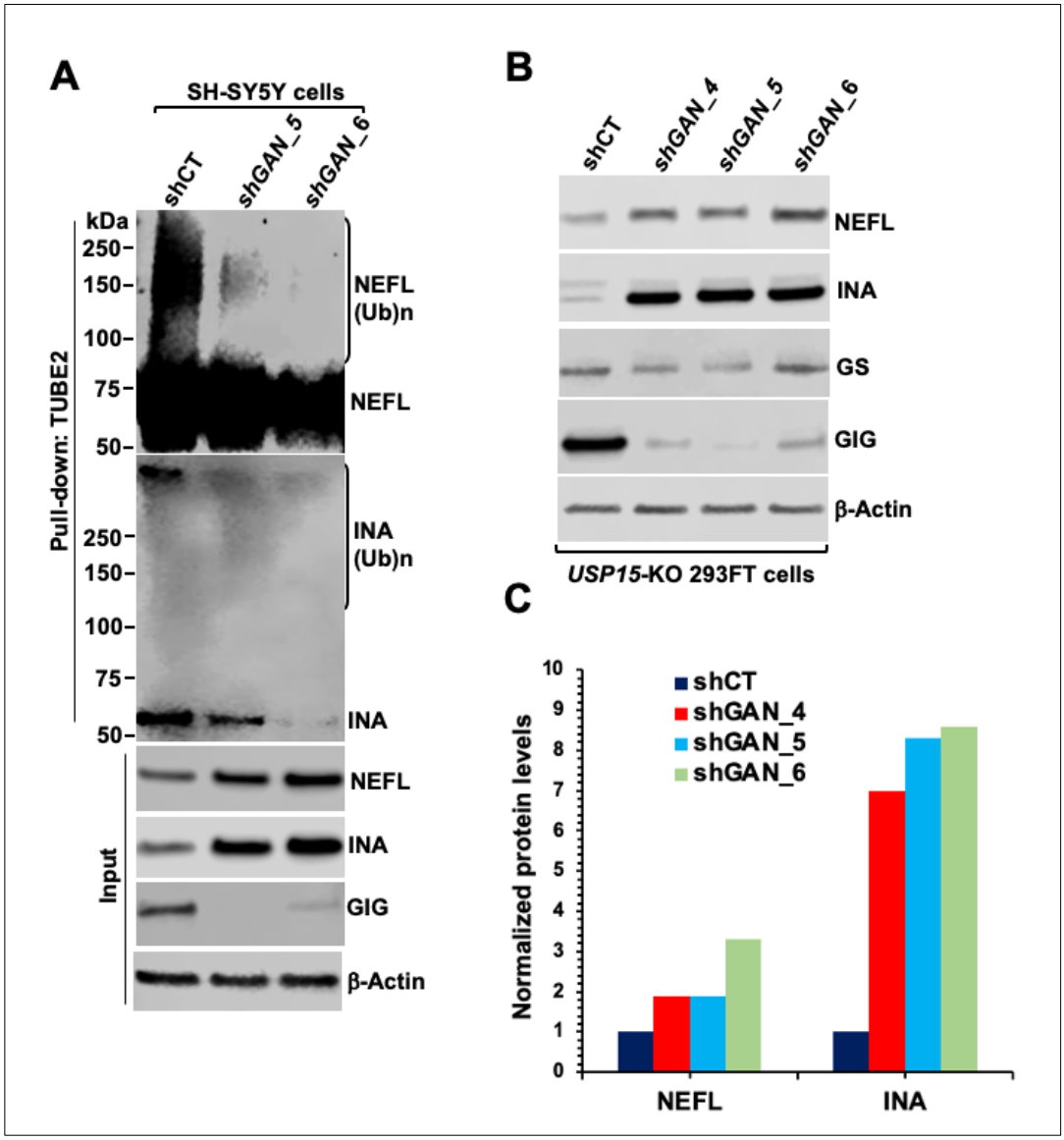

Fig. S10, Related to Fig. 3. USP15 regulates the stability of NEFL and INA proteins by acting downstream of CRL3^{GIG}.

(A) Total ubiquitylated proteins, extracted from SH-SY5Y cells stably expressing non-target shRNA lentivirus (CT) or GIPZ lentiviral shRNA targeting human *GAN* clones 5 and 6, were purified using TUBE2-agarose. Bound fractions and inputs were analyzed by IB with antibodies against NEFL, INA, GIG and Actin. (Ub)n, polyubiquitin.

(B) Cell lysates were extracted from *USP15*-KO 293FT cells stably expressing shRNA control (shCT) and shRNAs targeting *GAN* clones 4, 5, and 6 (shGAN_4, shGAN_5, shGAN_6) and were analyzed by IB with the indicated antibodies. (C) Quantification of NEFL and INA proteins from (B). Data are representative of two independent experiments (A & B).

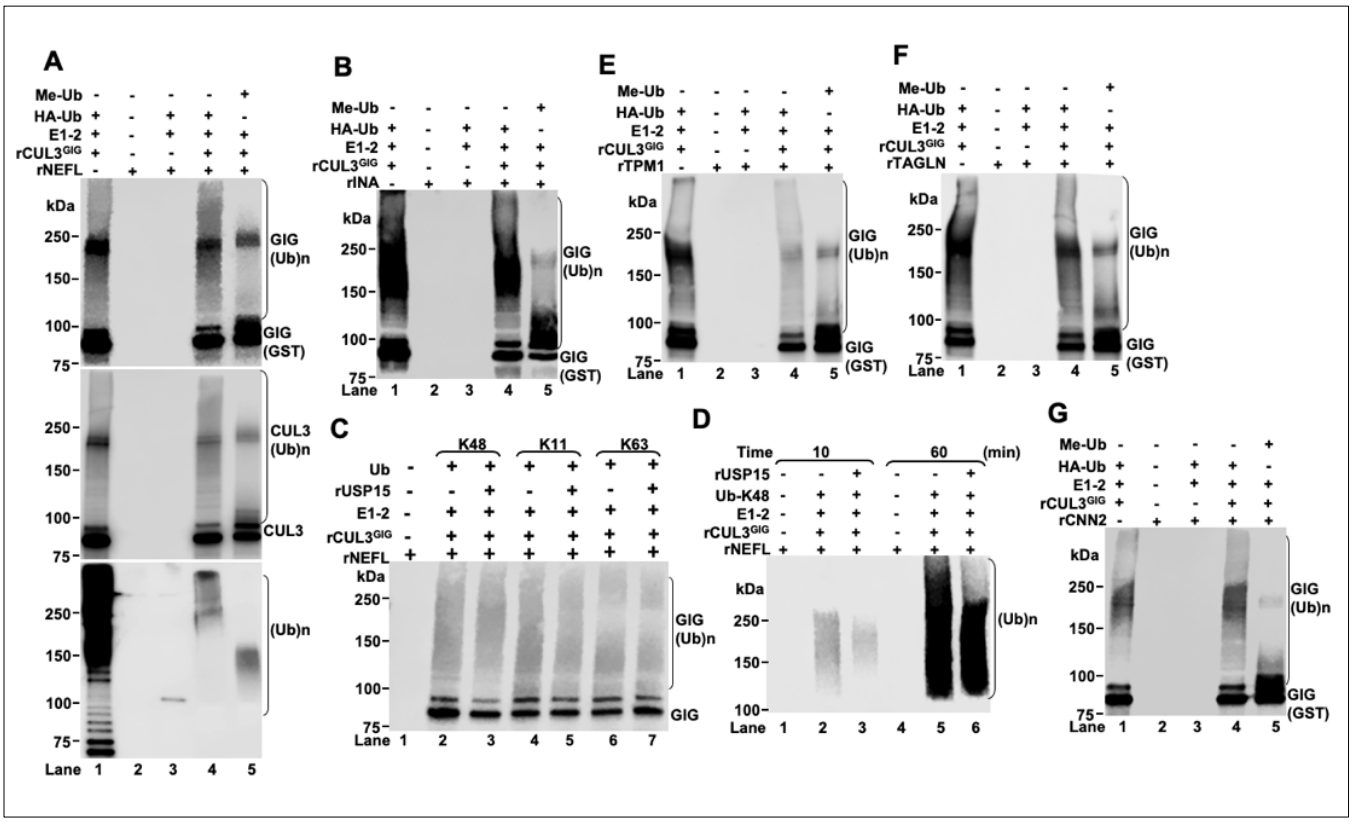

Fig. S11, related to Fig. 3. CRL3^{GIG} directly ubiquitylates NF proteins and actin filament-binding regulatory proteins in vitro. Fig. S11A, B, C, D, E, F and G are related to Fig. 3G, H, I, J, K, L, and M, respectively. In vitro ubiquitylation reactions of rNEFL (A), rINA (B); rTPM1 (E), rTAGLN (F), rCNN2 (G), and (C-D) In vitro competitive ubiquitylation/deubiquitylation assay of NEFL.

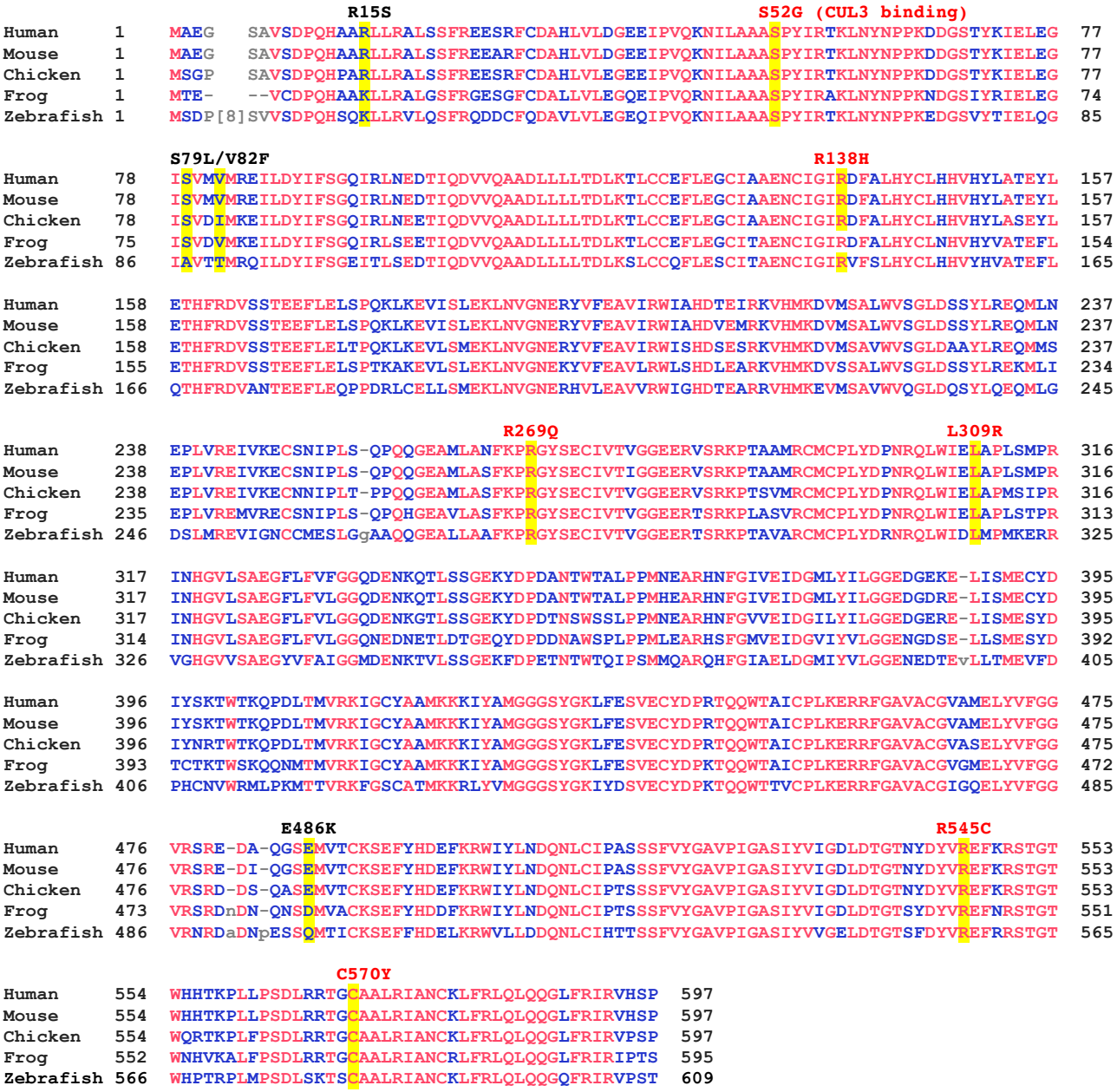

Fig. S12, related to Fig. 4. The sequence alignment of Gigaxonin orthologs across species. Multiple mutations in human GAN patients (1, 2), which are highlighted in yellow, were shown.
This is a graphic representation of amino acid sequence alignment, generated using COBALT. NP_071324.1: gigaxonin isoform 1 (Homo sapiens); NP_001074620.1: gigaxonin (Mus musculus); XP_428110.3: gigaxonin isoform X1 (Gallus gallus); NP_001016530.1: gigaxonin (Xenopus tropicalis); XP_003200482.3 gigaxonin (Danio rerio).

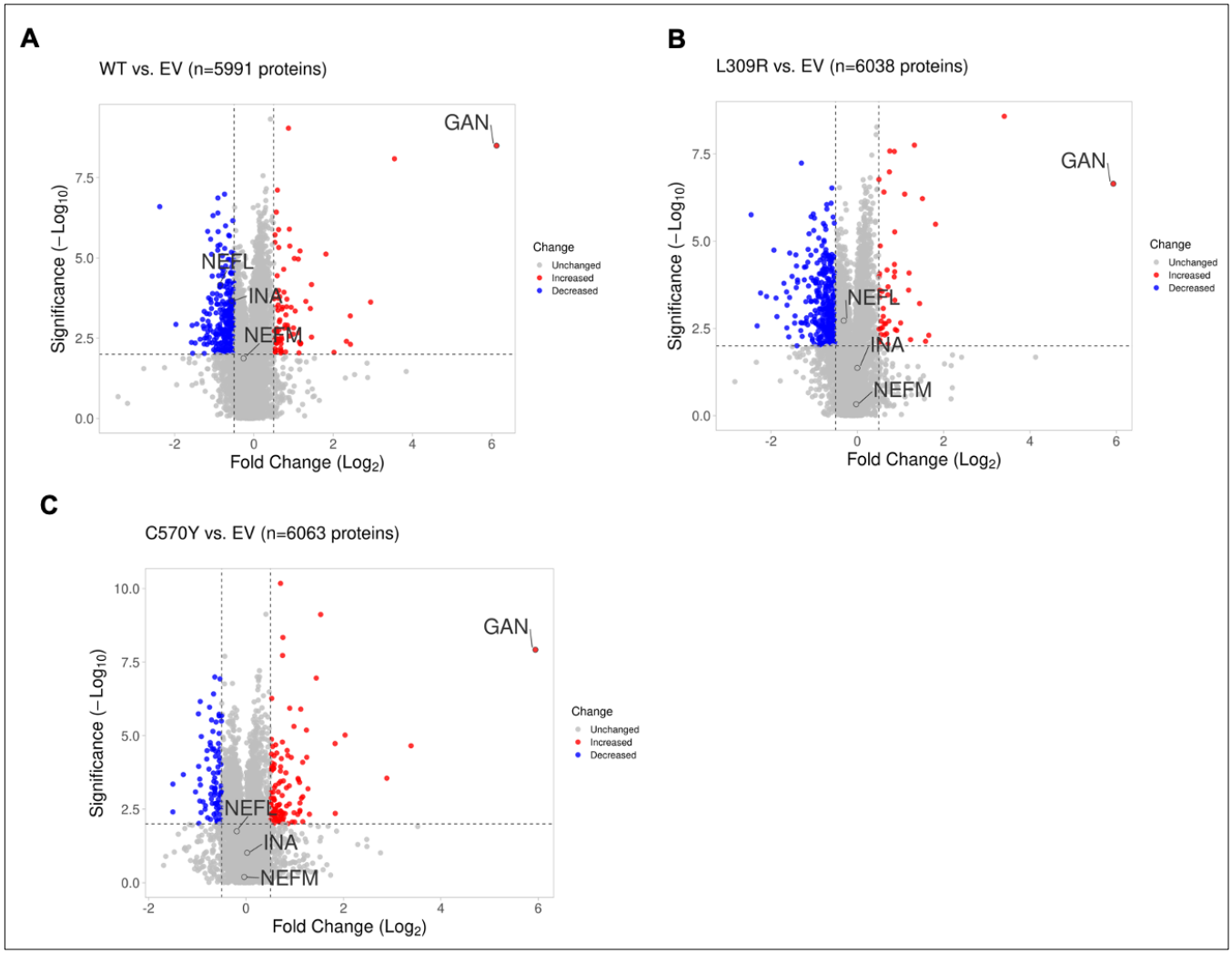

Fig. S13, Related to Fig. 4. (A-C) Global proteome analyses (n = 3) of EV-, WT GIG^{FLAG}-, L309R mutant- and C570Y mutant-transfected *GAN*-KO 293FT cells. The threshold of fold changes was set to more than 1.41-fold increase or decrease, and the $-Log_{10}$ p-value above 2. The data were depicted as volcano plots for WT vs EV (A), L309R vs EV (B), and C570Y vs EV (C). The red and blue dots denote significantly enriched or reduced proteins, respectively.

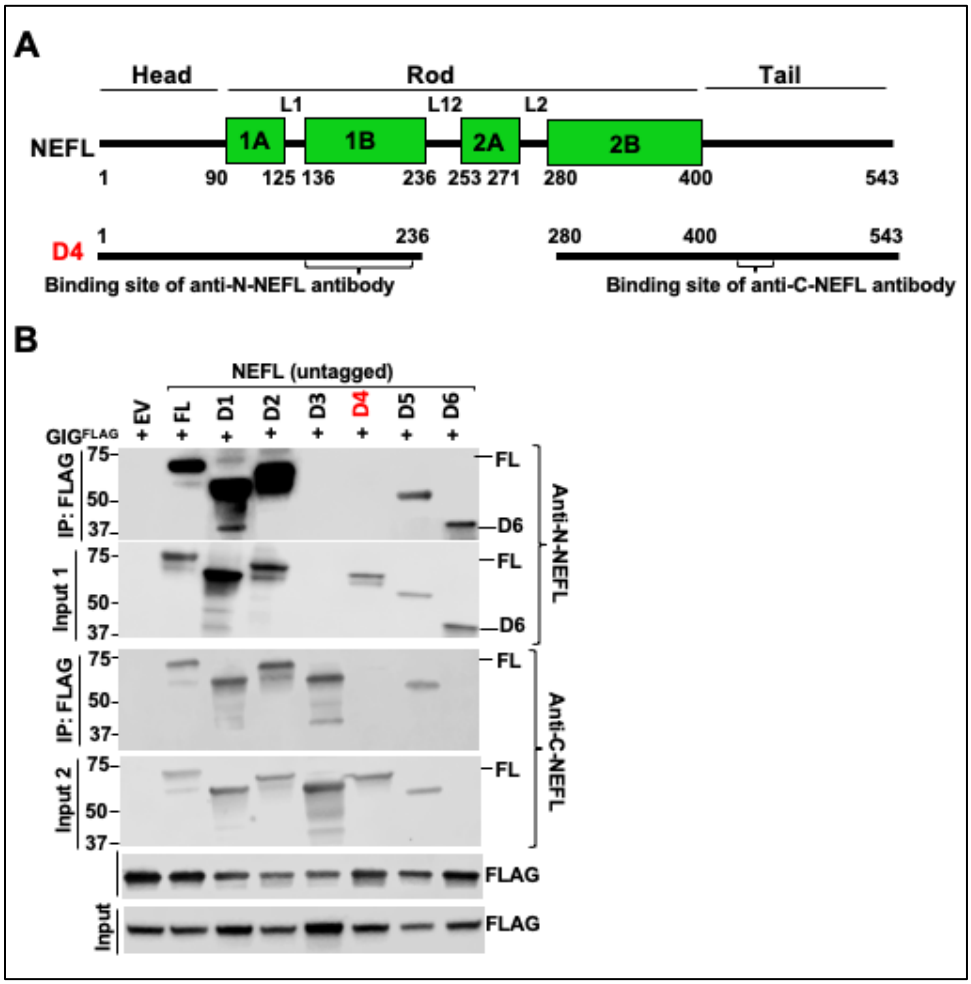

Fig. S14, Related to Fig. 5. (A) Schematic diagram of human NEFL protein and D4 deletion mutant. (B) 293FT cells were transfected with the indicated plasmids expressing GIG^{FLAG} and full-length (FL) or deletions of untagged NEFL (D1-6) for 40 h. Cellular extracts were immunoprecipitated with anti-Flag antibody, followed by immunoblotting with anti-N-NEFL antibody (Immunogen contains a sequence corresponding to amino acids 60-250, 3L9Y10), which does not bind to D3 as shown in Input 1, and anti-C-NEFL antibody produced by using a synthetic peptide surrounding Glu450 of NEFL in the C-terminal tail (C28E10), which does not bind to D6 as shown in Input 2; n = 2.

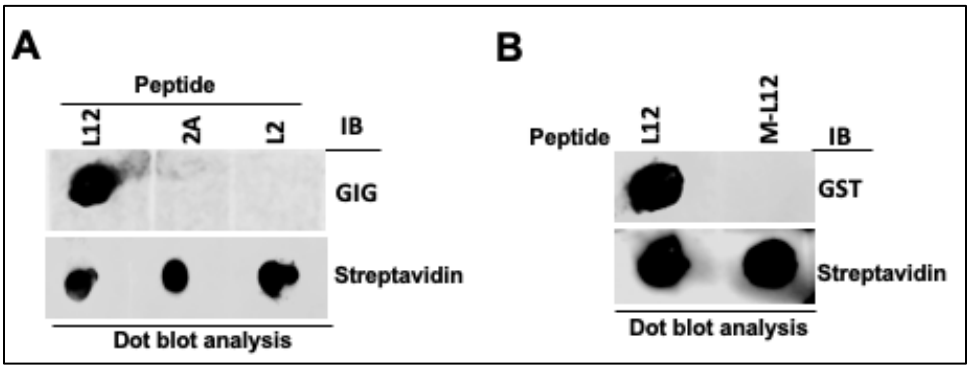

Fig. S15, Related to Fig. 5. Peptide NEFL-L12 interacted with rGIG protein in dot blot assays. (A) Dot blot analysis was done using ^{GST}GIG protein and immobilized NEFL-L12, -2A and –L2 peptides, followed by IB with anti-GIG and streptavidin-HRP antibodies. (B) Dot blot analysis was done using ^{GST}GIG protein and immobilized NEFL-L12, and NEFM-L12 (M-L12) peptides, followed by IB with anti-GST and streptavidin-HRP antibodies. At least three independent experiments were repeated (A & B).

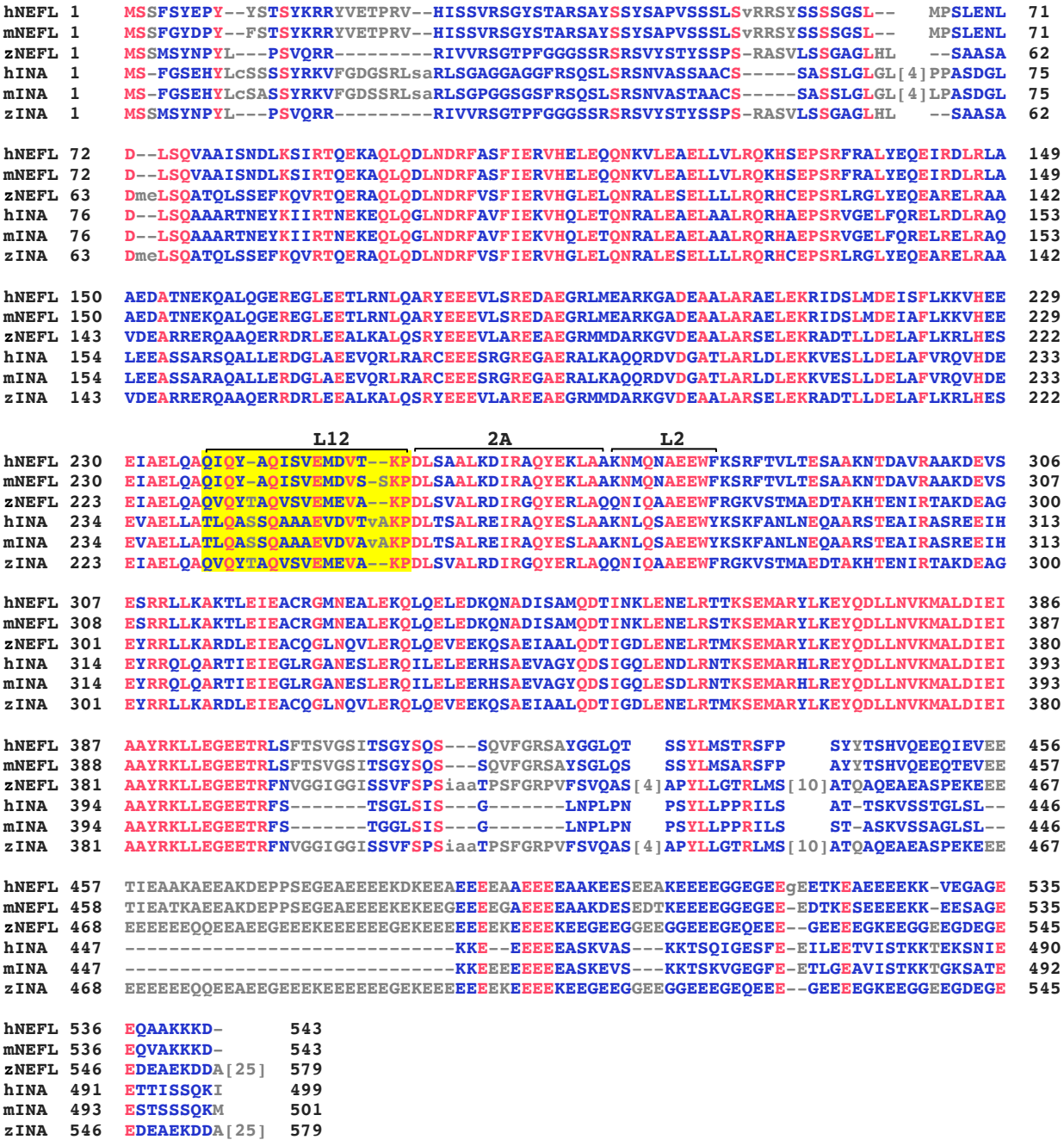

Fig. S16, Related to Fig. 5. (A) The sequence alignment of human (h), mouse (m) and zebrafish (z) NEFL and INA orthologs. The L12 region was highlighted in yellow.

Supplemental Tables

A

Protein names	Fold change[a]	ms/ms count		P-value
		293FT WT	USP15 -KO	
Glutamine synthetase (GS)	0.57	24	20	7.7 E-06
Arginyl-tRNA--protein transferase 1	0.53	35	12	3.2 E-03
Ribonuclease T2	0.52	33	26	1.3 E-03
Acyl-coenzyme A thioesterase 1;Acyl-coenzyme A thioesterase 2, mitochondrial	0.50	71	44	1.5 E-04
Neurofilament light polypeptide (NEFL)	0.49	102	56	2.2 E-04
Cellular retinoic acid-binding protein 2	0.47	88	20	8.6 E-06
Phospholipid-transporting ATPase IG	0.47	36	21	3.1 E-03
Microsomal glutathione S-transferase 1	0.46	62	33	3.8 E-04
Alpha-internexin (INA)	0.27	40	12	7.9 E-06
DNA damage-regulated autophagy modulator protein 2	0.17	308	343	2.7 E-04
Ubiquitin carboxyl-terminal hydrolase 15 (USP15)	0.0085	51	2	4.8 E-09

[a] Peptide intensity quantification based on Label Free Quantification (LFQ)

Glutamine synthetase is an endogenous substrate of USP15, which was identified in a recent study (3).

B

Protein names	Fold change [b]	ms/ms count		P-value
		293FT WT	USP15-KO	
G protein-regulated inducer of neurite outgrowth 1	2.12	16	35	1.3 E-04
Nuclear ubiquitous casein and cyclin-dependent kinase substrate 1	2.04	30	49	5.1 E-04
Zinc finger protein 609	1.89	4	19	7.8 E-04
Transcription factor Dp-1	1.81	19	30	2.0 E-04
Thymidylate synthase	1.80	36	50	3.7 E-06
S-phase kinase-associated protein 2	1.77	39	53	5.3 E-07
Genetic suppressor element 1	1.74	16	25	1.2 E-04
Hydroxymethylglutaryl-CoA synthase, cytoplasmic	1.65	123	155	1.3 E-03
Cullin-4A	1.63	51	95	1.1 E-04
Synaptosomal-associated protein 23	1.63	37	71	1.4 E-03

[b] Peptide intensity quantification based on Label Free Quantification (LFQ)

Table S1. Down-regulated proteins (A) and up-regulated proteins (B) in *USP15*-KO 293FT cells

A

i	Volume	Hydrophobicity	Buriedness	Aromatic	DLID	Area
1	1131.345215	0.610956	0.841242	0.008025	1.192476	819.598816
3	476.130035	0.604139	0.818425	0	0.448121	426.674408
2	396.803589	0.483356	0.689081	0	-0.4702244	425.984009
4	308.369598	0.515483	0.725865	0.007286	-0.4385237	309.504486
5	203.957474	0.54148	0.699552	0	-0.7883903	250.560165
8	177.687576	0.452381	0.70028	0	-1.089575	205.481216
6	172.252975	0.602757	0.803258	0.02381	-0.3654213	226.338043
7	165.916504	0.549731	0.717742	0	-0.8503947	205.274612
9	148.801636	0.401786	0.623512	0	-1.637876	188.867233
11	144.84671	0.699203	0.842629	0	-0.1193039	146.028885
13	115.252693	0.575472	0.834906	0	-0.5993441	121.523628
10	109.302483	0.433206	0.578244	0	-1.972669	146.06958

B

E3	HBOND	HPHOB	VWINT	DOCKING SCORE
WILDTYPE	-11.07097	-9.437644	-60.10344	-9.660122
C570Y	-13.5544	-9.592851	-53.94953	-4.920272

Table S2: The pockets are scored based on several factors, such as size, shape, and electrostatic properties. (A) Pocket 1 in the C-terminal Kelch domain of GIG has the best drug like density (DLID) score and is highlighted in dark blue. It was selected as a target for local docking with the NEFL-L12 peptide (the $NEFL^{L12}$ degron: **QISVEMDV**). (B) Comparison of docking score between wild-type Gigaxonin and its C570Y mutant.

Table S3. Key reagents used in this study.

Designation	Source	Identifier
Chemical compounds & reagents		
Bortezomib	Thermo Fisher Scientific	50-741-9
Pevonedistat (MLN4924)	Selleck Chemicals	S7109
Cycloheximide (CHX)	Sigma	C7698
Fugene HD	Promega	E2311
Antibodies		
Anti-USP15 antibody	Abnova	1C10, H00009958-M01
Anti-Gigaxonin Antibody for IP	Novus Biologicals	NBP1-49924
Anti-Gigaxonin Antibody (F-3) for IB	Santa Cruz Biotechnology	sc-376173
Normal rabbit IgG control for IP	Santa Cruz Biotechnology	sc-3888
Anti-USP11 Antibody (C-6)	Santa Cruz Biotechnology	sc-365528
Anti-USP7/HAUSP Antibody (H-12)	Santa Cruz Biotechnology	sc-137008
Anti-CUL-3 Antibody (G-8)	Santa Cruz Biotechnology	sc-166110
Anti-glutamine synthetase	Santa Cruz Biotechnology	sc-74430
Anti- Ubiquitin Antibody (P4D1) HRP	Santa Cruz Biotechnology	sc-8017 HRP
Anti-NF-M (NEFM) Antibody (1A2)	Santa Cruz Biotechnology	sc-20013
Anti-NEFL mAb (3L9Y10); detect N-terminal	Thermo Fisher Scientific	MA5-42752
Anti-GST-HRP antibody	Thermo Fisher Scientific	MA4-004-HRP
Anti-NEFL (C28E10) mAb (detect C-terminal)	Cell Signaling Technology	2837
alpha-internexin (INA) antibody	Cell Signaling Technology	77024
Anti-Streptavidin-HRP	Cell Signaling Technology	3999S
Anti-TPM1 antibody	Novus Biologicals	NBP2-75689
Anti-CNN2 Antibody	Novus Biologicals	NBP2-13848
Anti-TPM2 antibody	Proteintech	11038-1-AP
Anti-TAGLN antibody	Proteintech	10493-1-AP
Anti- BRMS1 antibody	Proteintech	16096-1-AP
anti-β-Actin-HRP	Abcam	ab49900
Anti-Flag HRP	Sigma	SAB5300168

Anti-Myc HRP	Sigma	16-213
Anti-Flag HRP	Rockland Immunochemicals	600-403-383
HRP Goat Anti-Rabbit IgG	Vector Laboratories	PI-1000-1
HRP Horse Anti-Mouse IgG	Vector Laboratories	PI-2000-1
IP and pulldown beads		
Anti-c-Myc Affinity Gel	Sigma	E6654
Anti-Flag M2 Affinity Gels	Sigma	F2426
Protein G agarose	Sigma	16-266
TUBE2 (Agarose)	LifeSensors	UM402
Dynabeads M-280 streptavidin	Thermo Fisher Scientific	11205D
Recombinant Proteins		
Human His6-USP15	R&D Systems	E-594
Recombinant Human His6CUL3/NEDD8/RBX1 Complex Protein	R&D Systems	E3-436
Recombinant Human Gigaxonin GST Protein	Novus Biologicals	H00008139-P01
Recombinant Human NEFL protein	Abcam	ab224840
Recombinant Human alpha Internexin protein	Abcam	ab160346
Recombinant Human Tropomyosin-1 Protein	Novus Biologicals	NBP1-48329
Recombinant Human TAGLN His Protein	Novus Biologicals	NBP1-45267
Recombinant Human Calponin-2(CNN2)	CUSABIO	CSB-EP860764HU
Ubiquitin Activating Enzyme/UBE1	BostonBiochem	E-305
Human UbcH5a	BostonBiochem	E2-616
Human His6 UbcH3	BostonBiochem	E2--610
Human HA Ubiquitin	BostonBiochem	U-110
His6-Ubiquitin Mutant with K48 only,	R&D Systems	UM-HK480
His6-Ubiquitin Mutant with K11 only,	R&D Systems	UM-HK110
His6-Ubiquitin Mutant with K63 only,	R&D Systems	UM-HK630
Synthetic Peptides		
NEFL Peptides: L12: QIQYAQISVEMDVT-K-BIOTIN		Biomatik

2A: KPDLSAALKDIRAQYEKLAA-K-BIOTIN L2: KNMQNAEEWF-K-BIOTIN **NEFM-L12 Peptide:** M-L12: QIQASHITVERKD-K-Biotin		
Human cell lines		
293FT cells	Thermo Fisher Scientific	R70007
SH-SY5Y Cells	ATCC	CRL-2266
USP15-KO 293FT cells	In our recent study (3)	
GAN-KO 293FT cells	This study	
DNA Plasmids		
Gigaxonin CRISPR/Cas9 KO Plasmid (h2)	Santa Cruz Biotechnology	sc-407001-KO-2
Vector pcDNA3.1+/C-(K)-DYK with a C-terminal Flag tag, expressing human USP15 isoform 1 (NM_001252078.2): WT USP15-Flag and C298A-USP15-Flag (CA) mutant.		In a recent study (3).
GAN_ pcDNA3.1+/C-(K)DYK (FLAG)		GenScript
GAN_ pcDNA3.1+/C-(K)DYK (FLAG) mutants GAN-L309R GAN-E486K GAN-R545C GAN-C570Y		GenScript
NEFL_pcDNA3.1(+)-C-Myc vector		GenScript
NEFL_pcDNA3.1(+)-C-Myc vector (2A mutant: 246-EMD-248 mutated into 246-AMA-248)		GenScript
NEFL deletion mutants **with MYC Tag** from NEFL_OHu28006C_pcDNA3.1(+)-C-Myc (6 deletion mutants): 1- NEFL-D1: deletion of amino acids 2-90: deletion of head 2- NEFL-D2: deletion of amino acids 91-125: deletion of A1 3- NEFL-D3: deletion of amino acids 136-236: deletion of 1B 4- NEFL-D4: deletion of amino acids 237-279: deletion of L12 2A L2 5- NEFL-D5: deletion of amino acids 280-400: deletion of 2B 6- NEFL-D6: deletion of amino acids 400-543: deletion of tail		GenScript
NEFL WT or deletion mutants **without MYC Tag** from NEFL_OHu28006C_pcDNA3.1(+) (6 deletion mutants): 1- NEFL-D1: deletion of amino acids 2-90: deletion of head 2- NEFL-D2: deletion of amino acids 91-125: deletion of A1 3- NEFL-D3: deletion of amino acids 136-236: deletion of 1B 4- NEFL-D4: deletion of amino acids 237-279: deletion of L12 2A L2 5- NEFL-D5: deletion of amino acids 280-400: deletion of 2B 6- NEFL-D6: deletion of amino acids 400-543: deletion of tail		GenScript

GIPZ Lentiviral shRNA vectors targeting *USP15, reported in a recent study (3):* USP15_4 shRNA: V2LHS_13437. USP15_6 shRNA: V3LHS_336551.	Horizon Discovery
GIPZ Lentiviral Human USP11 shRNA, catalog # RHS4531-EG8237 (clones 1 - 5): RHS4430-200211208, RHS4430-200270438, RHS4430-200272001, RHS4430-200299663, RHS4430-200306337	Horizon Discovery
GIPZ Lentiviral Human USP7 shRNA, catalog # RHS4531-EG7874 (clones 1 - 3): RHS4430-200175624, RHS4430-200287423, RHS4430-200297458	Horizon Discovery
GIPZ negative (non-targeting or non-silencing) shRNA control	Horizon Discovery

Supplemental Materials and Methods

Immunoblot analysis, native and denaturing Immunoprecipitation (IP) and TUBE2 Pulldown

The protocols for immunoblot analysis and native immunoprecipitation (IP) and denaturing IP were described in our previous studies (4, 5). TUBE2 Pulldown experiments were described in our recent studies (3, 6).

Generation of stable cell lines expressing shRNAs targeting *USP15, USP7, USP15* and *GAN*

The protocols for the generation of stable cell lines using a lentiviral GIPZ shRNA system targeting *USP15, USP7, USP15* and *GAN* were described in our recent study (3).

Cycloheximide (CHX) Chase Experiments

CHX experiments were described previously (3, 5, 6).

RNA-sequencing (Seq) Analysis

WT, *USP15*-KO, *USP15*-KO (for MLN4924 treatment), *GAN*-KO2 293FT cells, seeded at $0.5x10^6$ cells/well in 6-well plates (biological triplicates for each experimental condition), were grown for 2 days. For MLN4924 treatment, USP15-KO 293FT cells treated with 1 μM MLN4924 for 8 h. Then, cells were harvested using trypsin and extensively washed at least 2 times with cold PBS. Cell pellets were snap-frozen in liquid nitrogen and stored at -80 ^{0}C. Total RNA was extracted using RNAeasy Mini Kit (QIAGEN 74104). RNA samples were further treated with RNase-Free TURBO™ DNase (2 U/μL) (Thermo Fisher, Catalog # AM2238) by mixing 95 μl total RNA + 10 μl of 10x Turbo DNase buffer + 1.5 μl RNA TURBO™ DNase at 37 ^{0}C for 30 min. DNase-treated samples were purified using RNAeasy Mini Kit (QIAGEN 74104). RNA was measured and diluted at 100 ng/μl.

RNA-Seq analysis was conducted at LC Sciences LLC (Houston, TX) using the 2×150bp paired-end sequencing (PE150) on an Illumina NovaseqTM 6000 following the vendor's recommended protocol. Differential gene expression analysis was performed by DESeq2 software between two

different groups (and by edgeR between two samples). The genes with the false discovery rate (FDR) parameter below 0.05 and absolute fold change ≥ 2 were considered differentially expressed genes.

Proteomic analysis of proteins in WT and *USP15*-KO 293FT cell lines

Cell culture. 293FT cells and CRISPR-Cas9 genome-edited USP15-KO 293FT cells were cultured in a 100-mm plate with the DMEM media supplemented with 10% fetal bovine serum (Gibco), penicillin streptomycin (Gibco cat# 15070063), and 2 mM L-glutamine (Gibco cat# 25030081). Each cell type was harvested after the cell confluency reached 80%. Harvested cells were stored at –70 ℃ for further preparations.

Sample preparation. Harvested 293FT and USP15-KO 293FT cells were lysed using 4% SDS buffer and sonicated for 10 min. Lysates (250 μg) were mixed with 200 μL of 8 M urea in 0.1 M Tris-HCl (pH 8.5), and digested for 18 h using the Filter Aided Sample Preparation (FASP) method (7) in 30-kDa Microcon filtration devices (Millipore). Trypsin (Promega cat# V5111) and Lys-C (Wako cat# 121-05061) were used at enzyme to protein ratio 1:100. After centrifugation, 100 μL of 0.05 M chloroacetamide in 8 M urea, 0.1 M Tris-HCl (pH 8.5) was added to the peptide mixture for 1 h. Digested peptides were divided into 7 fractions using mid-pH fractionation. Each fraction was eluted with 2%, 5%, 7.5%, 12.5%, 15%, 20%, and 80% acetonitrile mixed with mass spectrometry-grade water. Fractions were desalted using in-house StageTips (8) spin chromatography columns filled with 47 mm C18 extraction disks (Empore cat# 66883-U). All fractionated samples were concentrated using a vacuum concentrator for further analysis.

Liquid chromatography-mass spectrometry. Dried tryptic peptides were solubilized using 0.1% formic acid (Fisher cat# LS118). Mass spectrometric raw data was produced using an Ultra High-Resolution Tribrid Mass Spectrometer (Orbitrap Fusion Eclipse; Thermo cat# FNS04-10000) coupled with an EASY-nLC 1000 (Thermo Fisher Scientific). Each chromatogram was regulated by mobile phase A (0.1% formic acid, FA) and separated in mobile phase B (90% acetonitrile, 0.1% FA) through a 15-cm capillary column (75 μm internal diameter, in-house packed, filled with ReproSil-Pur C18-AQ-3-μm resin (Dr. Maisch GmbH)) using a 120-min gradient from 5% to 35% at an average flow rate of 600 nL/min. The mass spectrometer was set to a data-dependent mode with 2 seconds between each master scan cycle. Survey

scans were acquired at a resolution of 120,000 over 400–1600 m/z with an intensity range filtered between 5.0 e^3 to 1.0 e^{20}. Isolation was set to quadrupole mode with 1.2 m/z widths followed by higher energy collision dissociation-mediated fragmentation at 33% fixed energy. Peaks selected more than once within 20 s were excluded.

Mass spectrometry. Each tandem mass raw data analysis was searched against the UniProt human database (version 2022.02.23; contains 20,376 reviewed entries) using the MaxQuant software (9). Precursor mass and fragment ions mass errors were set to 4.5 ppm and 20 ppm. Carbamidomethylation of cysteine was set as a fixed modification. Variable modifications used in the initial proteome analysis consisted of methionine oxidation, protein N-terminal acetylation, and Gly-Gly motifs for ubiquitination sites. Protein quantification was filtered to match at least one razor peptide or unique peptide containing protein group, and at least two different ratio measurements for protein quantification. 'Re-quantify' function was applied for detailed identification options to minimize missed identifications (10). Further peptide and protein identifications were sorted at a 1% false discovery rate (FDR). Peptide intensity quantification was carried out by the Label Free Quantification (LFQ) method, with the default normalization values.

Protein identification and expression profile analysis was performed with the Perseus computational platform (version 2.0.7.0) (11). Identified proteins with flagged notions of 'reverse', 'only identified by site', and non-human 'contaminants' were excluded from the list for initial analysis. Differential expressed protein selection was done by log2 transforming of the LFQ intensity. The protein groups quantified in all the replicates were used for a paired t-test. P-values less than 0.010, and log2 fold changes above 1 and below –1 were regarded as statistically significant and differential expressed proteins. Among the list, protein validity scores above 100 previously calculated by the MaxQuant software were further emphasized as highly potential target proteins.

Quantitative proteomic analysis of proteins in WT and *GAN*-KO 293FT cell lines

Using a 10plex Tandem Mass Tag (TMT) workflow, we utilized multiplexed quantitative proteomics on total-cell extracts. The proteome profiling was performed as described recently (12). Briefly, WT (4 replicates), and *GAN*-KO2 and *GAN*-KO16 293FT cell lines (triplicate each) were prepared. Each sample was split in half and flash-frozen in liquid N_2. One-half of each sample was analyzed by immunoblotting (IB), and the other half was used for the whole proteome analysis. Briefly, 100 μg of protein per sample was digested with Trypsin and labeled with isobaric 10plex TMT reagents before combining them. MS data were collected using real-time search TMT-MS^3 method (13) on an Orbitrap Eclipse Tribrid mass spectrometer equipped with the FAIMS Pro Interface (14). The resulting raw data files were processed using a Comet-based software pipeline, MassPike, and peptide sequences search against the Human Reference Proteome UniProt database (SwissProt database downloaded on 2020-03 containing canonical and isoform entries as well as a curated list of common contaminants). Relative protein quantification based on signal-to-noise TMT-based reporter ion quantitation was computed and exported to Excel, and downstream statistical analysis was performed using R and Perseus software. The designed experiment with quadruplicate quantitative measurement aimed to provide ideal statistical power for identifying GIG substrates and the usage of two independent KO clones to mitigate possible CRISPR-Cas9 and clonal off-target effects.

Quantitative proteomic analysis of proteins in *GAN*-KO 293FT cells transiently transfected with empty vector (EV, control), WT GIG^{FLAG}, L309R and C570Y mutants

GAN-KO 293FT cells, cultured in 10-cm plates overnight (60% confluence), were trans transiently transfected with EV, WT GIG^{FLAG}, L309R or C570Y mutant (6 μg/plate, each had 4 plates: 1 for Western blotting analysis, and 3 others for proteomic study/triplicate). After transfection of 40-48 h, cells were harvested using trypsin, neutralized with complete medium 10% FBS. Cells were washed extensively 4 times with cold PBS and snap frozen with liquid nitrogen before being stored at -80 ^{0}C until use. Cell pellets were lysed with 1 ml (each sample) of 4% SDS/50 mM Tris, pH 7.5-8.0 and 5mM DTT, boiled for 5 min and briefly sonicated. Cell lysates were centrifuged to remove cell debris, precipitated with 4 volumes of cold acetone, and stored at -20 ^{0}C overnight. Protein pellets were recovered by centrifugation

at 16.1k x g for 10 min at 4°C and washed by 80% acetone once. The final protein pellets were suspended in 6M urea, 2M thiourea and 100mM ammonium bicarbonate. The protein concentration was determined using Pierce 660nm Protein Assay (Thermo Fisher Scientific) according to the manufacturer's protocol. 50 microgram proteins from each sample were reduced by 5 mM dithiothreitol (DTT) at room temperature for 1hr and alkylated by 15 mM iodoacetamide (IAA) at room temperature for 30 min in the dark. The excess of IAA was quenched by adding 5mM DTT and incubate for 15 min. Mass spectrometry-grade LyC (NEB) was added at an enzyme-to-protein ratio of 1:50 (w/w) and incubated for 3 h at 37 °C, and mass spectrometry-grade trypsin at a 1:50 (w/w) ratio was added for digestion overnight at 37 °C. Digestion was quenched with 1% FA. For experimental DDA library generation, 8 micrograms protein digests from each sample were pooled and loaded onto a high-pH RP fractionation spin column (Pierce) according to the manual instruction. Eight fractionated peptide samples were dried and dissolved in 0.1% FA. Peptide concentrations were measured optically at 280 nm (Nanodrop 2000; Thermo Fisher Scientific), and 400 ng peptides were loaded onto Evotips for LC–MS/MS analysis. The Evosep One LC system coupled with a timsTOF Pro2 mass spectrometer (Bruker) was used to measure all samples. We used the 30 SPD (samples per day) method on a 15 cm × 150 µm column with 1.5 µm C18-beads (PepSep) at 40 °C. The analytical columns were connected with a fused silica ID emitter (10 µm ID; Bruker Daltonics) inside a nanoelectrospray ion source (Captive spray source; Bruker). The mobile phases comprised 0.1% FA as solution A and 0.1% FA/99.9% ACN as solution B.

The library samples were acquired using the DDA-PASEF mode, with one MS frame and 10 PASEF/MSMS scans per topN acquisition cycle. Precursors with a charge of +1 were filtered out based on their position in the m/z-IM plane, and only precursors with an intensity threshold of 2500 arbitrary units were selected for fragmentation. Target MS intensity for MS was set at 10,000 arbitrary units, ion mobility coefficient (1/K0) value was set from 1.6 to 0.6 V cm^{-2}, collision energy was set from 20-59 eV, MS data were collected over m/z range of 100 to 1700. Dynamic exclusion was activated after 0.4 minutes, and isolation width was set to 2 for m/z <700 or 3 for m/z >700. PydiAID-optimized dia-PASEF method was used to cover an m/z range from 300 to 1200 for proteome analysis (15). The method included two IM windows per dia-PASEF scan with variable isolation window widths adjusted to the

precursor densities from experimental spectral library. A total of 25 dia-PASEF scans were performed at a throughput of 30 SPDs, with a cycle time of 2.7 seconds.

For comparative analysis, we employed Spectronaut version 17.1 and utilized the default search unless otherwise indicated. All data were searched against the reviewed human proteome (UniProt, UP000005640), which contained 20,360 entries without isoforms, using trypsin/LysC as the digestion enzymes. Cysteine carbamidomethylation was set as a fixed modification, while methionine oxidation and acetylation at the N-terminus were selected as variable modifications. A maximum of two missed cleavages and up to three variable modifications was allowed. The FDR cutoff was established at 1%, while the precursor peptide and q-value cutoffs were set at 0.2 and 0.01, respectively. In addition, protein q-value experiment and run-wide cutoffs were determined to be 0.01 and 0.05, respectively. Single hit proteins by stripped sequence were excluded. Protein quantification was performed by filtering precursors using a sparse q-value approach, without the use of imputation. The prototypicity filter was set to only protein group specific peptides. Protein quantification was done using MaxLFQ based on the area of MS2, with cross-run normalization enabled. Differential abundance testing was performed using unpaired t-tests. In our analysis, we used a significance threshold of p-value < 0.01, an FDR < 0.05, and an absolute average log2 (fold change) > 0.5 to identify significant candidates. These criteria were applied to select the most promising candidates for further investigation.

Peptide pull-down and dot blot assays

The peptide pull-down assay was performed as described previously (5). Briefly, biotinylated NEFL and NEFM peptides were synthesized (Biomatik). Peptides (2 μg) were incubated with ^{GST}GIG (1 μg) or GIG^{FLAG} purified from transfected *GAN*-KO 293FT cells in 1 ml binding buffer (10 mM Tris [pH 7.6], 150 mM NaCl, 0.1% Triton X-100) containing a protease inhibitor cocktail and 1 mM DTT for 1-2 h at 4 ^{0}C. Then, M-280 streptavidin Dynabeads (20 μl) were washed and mixed with the peptide-protein complex for 1 h at 4 ^{0}C. After binding, the beads were washed 4 times in binding buffer. The bound proteins were eluted in 2x SDS loading buffer and analyzed by immunoblot. The dot blot assays were performed by spotting slowly 3 μl of diluted peptides (0.1 μg/μl in PBS) onto the nitrocellulose membrane

and letting it dry for 1-2 h. The membrane was blocked with 5% non-fat milk in TBST for 2 h, rinsed it with TBST for 1 min and probed with 1 μg recombinant ^{GST}GIG in 0.5 ml binding buffer. After 1 h, the membrane was washed extensively with TBST and analyzed by immunoblotting with the indicated antibodies.

Modelling and in silico study of the NEFL^{L12} degron (QISVEMDV) binding to Gigaxonin (GIG)

The amino acid sequence of Gigaxonin (known as KLHL16) encoded by the *GAN* gene (Homo sapiens, NP_071324, isoform 1; 597 aa) was used to build a model of the protein's 3D structure using Alphafold2, as described previously (16). Alphafold refines the initial model by iteratively minimizing a predicted energy function that takes into account factors such as steric clashes and electrostatic interactions. The full-length 3D structure of Gigaxonin in apo form was used to predict binding sites. ICM (Internal Coordinate Mechanics) Pocket Finder was used for predicting and analyzing protein-ligand interactions. The ICM Pocket Finder works by analyzing the protein structure and identifying regions where a ligand may bind or dock (17). The method is used, based on the principles of molecular mechanics, which use computational algorithms to calculate the energy of a molecular system and predict its behavior. First, the protein structure is prepared by adding missing atoms, assigning charges, and optimizing hydrogen bonding. After that, the software identifies potential binding pockets on the protein surface using a series of algorithms that analyze the shape and electrostatic properties of the protein surface.

The docking procedure started with Peptide Conformational Search. ICM uses an internal coordinate mechanics algorithm to generate multiple conformations of the peptide that are energetically favorable. After that, ICM performs docking calculations by sampling the orientations and conformations of the peptide in the binding site and scoring them based on various energy terms. After an initial docking is performed, the docking solutions are refined using a minimization algorithm that optimizes the intermolecular interactions between the protein and peptide. Docking score was calculated using biased probability Monte Carlo conformational searches and electrostatic calculations for peptides and proteins

(18). Finally, the docking results can be analyzed using various visualization tools including pymol and ICM MolSoft to examine the predicted binding modes and interactions between the protein and peptide.

Legends for Datasets S1 to S6

Dataset S1 (separate file), related to Fig. 1 & Table S1. Global Quantitative Proteomic Analysis of *USP15*-KO 293FT cells.
Dataset S2 (separate file), related to Fig. S3. RNA-Seq analysis of U*SP15*-KO 293FT cells.
Dataset S3 (separate file), related to Fig. S4. RNA-Seq analysis of MLN4924-treated *USP15*-KO 293FT cells.
Dataset S4 (separate file), related to Fig. 2. Global Quantitative Proteomic Analysis of *GAN*-KO 293FT cells.
Dataset S5 (separate file), related to Fig. 2. RNA-Seq analysis of *GAN*-KO 293FT cells.
Dataset S6 (separate file), related to Fig. 4 and Fig. S13. Global Quantitative Proteomic Analysis of *GAN*-KO 293FT cell lines, transfected with EV, WT GIG^{FLAG}, L309R and C570Y mutants.

SI References

1. P. Genschik, I. Sumara, E. Lechner, The emerging family of CULLIN3-RING ubiquitin ligases (CRL3s): cellular functions and disease implications. *EMBO J* **32**, 2307-2320 (2013).
2. P. Bomont *et al.*, The gene encoding gigaxonin, a new member of the cytoskeletal BTB/kelch repeat family, is mutated in giant axonal neuropathy. *Nat Genet* **26**, 370-374 (2000).
3. T. V. Nguyen, USP15 antagonizes CRL4(CRBN)-mediated ubiquitylation of glutamine synthetase and neosubstrates. *Proc Natl Acad Sci U S A* **118** (2021).
4. T. Van Nguyen *et al.*, SUMO-specific protease 1 is critical for early lymphoid development through regulation of STAT5 activation. *Mol Cell* **45**, 210-221 (2012).
5. T. V. Nguyen *et al.*, Glutamine Triggers Acetylation-Dependent Degradation of Glutamine Synthetase via the Thalidomide Receptor Cereblon. *Mol Cell* **61**, 809-820 (2016).
6. T. V. Nguyen *et al.*, p97/VCP promotes degradation of CRBN substrate glutamine synthetase and neosubstrates. *Proc Natl Acad Sci U S A* **114**, 3565-3571 (2017).
7. J. R. Wisniewski, A. Zougman, N. Nagaraj, M. Mann, Universal sample preparation method for proteome analysis. *Nat Methods* **6**, 359-362 (2009).
8. J. Rappsilber, M. Mann, Y. Ishihama, Protocol for micro-purification, enrichment, pre-fractionation and storage of peptides for proteomics using StageTips. *Nat Protoc* **2**, 1896-1906 (2007).
9. C. Wichmann *et al.*, MaxQuant. Live enables global targeting of more than 25,000 peptides. *Molecular & Cellular Proteomics* **18**, 982-994 (2019).
10. J. Cox *et al.*, A practical guide to the MaxQuant computational platform for SILAC-based quantitative proteomics. *Nat Protoc* **4**, 698-705 (2009).
11. S. Tyanova *et al.*, The Perseus computational platform for comprehensive analysis of (prote) omics data. *Nature methods* **13**, 731-740 (2016).
12. A. Ordureau *et al.*, Temporal proteomics during neurogenesis reveals large-scale proteome and organelle remodeling via selective autophagy. *Mol Cell* **81**, 5082-5098 e5011 (2021).
13. D. K. Schweppe *et al.*, Full-Featured, Real-Time Database Searching Platform Enables Fast and Accurate Multiplexed Quantitative Proteomics. *J Proteome Res* **19**, 2026-2034 (2020).
14. D. K. Schweppe *et al.*, Characterization and Optimization of Multiplexed Quantitative Analyses Using High-Field Asymmetric-Waveform Ion Mobility Mass Spectrometry. *Anal Chem* **91**, 4010-4016 (2019).
15. P. Skowronek *et al.*, Rapid and In-Depth Coverage of the (Phospho-)Proteome With Deep Libraries and Optimal Window Design for dia-PASEF. *Mol Cell Proteomics* **21**, 100279 (2022).
16. J. Jumper *et al.*, Highly accurate protein structure prediction with AlphaFold. *Nature* **596**, 583-589 (2021).

17. J. An, M. Totrov, R. Abagyan, Pocketome via comprehensive identification and classification of ligand binding envelopes. *Mol Cell Proteomics* **4**, 752-761 (2005).
18. R. Abagyan, M. Totrov, Biased probability Monte Carlo conformational searches and electrostatic calculations for peptides and proteins. *J Mol Biol* **235**, 983-1002 (1994).